

Investigating Levy's model in financial series prediction (case of vanilla option)

Seyed Jalal Tabatabaei¹

¹ Department of Management, Payamenoor University, Tehran, Iran
tabatabaei@pnu.ac.ir

Abstract:

In recent years, there has been growing interest in the application of stochastic processes to model financial markets, particularly in the pricing and prediction of derivative instruments such as options. One of the more advanced models that has emerged for capturing the dynamics of financial time series is the Lévy process, which generalizes the traditional Brownian motion by incorporating jumps and heavy tails, features often observed in real financial data. This paper investigates the applicability of Lévy processes in predicting the evolution of financial series, with a specific focus on vanilla option pricing. In our methodology, by reviewing the theoretical underpinnings of Lévy processes, highlighting key aspects such as the characteristic function and the variance-gamma process, we calibrate a Lévy-based model to 77 mid-prices of a set of European call options on the S&P 500 Index at the close of the market on 11 April 2022. We employ maximum likelihood estimation (MLE) and the expectation-maximization (EM) algorithm to fit the parameters of the Lévy process. Our results indicate that the Lévy process model provides a significantly better fit to market data than the Black-Scholes model, particularly in capturing the heavy tails and jump behavior observed in option price movements. Additionally, the Lévy model demonstrates superior predictive performance in out-of-sample testing, improving the accuracy of option pricing and hedging strategies. These findings suggest that Lévy processes hold substantial promise for enhancing financial series prediction and derivative pricing in markets characterized by volatility clustering and sudden jumps.

Keywords: Stochastic Processes, Brownian Motion, Poisson Process, Fourier Transform, Lévy-Khinchine Formula.

JEL Classifications: C02, C53, C65

1 Introduction

In the realm of financial markets, the precise modeling of asset price behavior is crucial for the valuation of derivative instruments, especially vanilla options. The Black-Scholes-Merton (BSM) model, developed by Black and Scholes (1973) alongside Merton (1973), posits that asset prices adhere to a geometric Brownian motion (GBM) characterized by continuous trajectories and constant volatility [7]. Although this model is mathematically sophisticated and serves as a cornerstone of contemporary financial theory, it exhibits notable deficiencies when applied to ac-

¹Corresponding author

Received: 28/08/2024 Accepted: 04/11/2024

<https://doi.org/10.22054/JMMF.2024.81540.1144>

tual market scenarios. Research conducted by Fama (1965) and Mandelbrot (1963) has repeatedly demonstrated that asset returns diverge from the normal distribution assumed by the BSM model, displaying traits such as fat tails, skewness, and abrupt jumps [15]. These deviations become particularly evident during periods of market turbulence, where abrupt and significant price fluctuations can lead to considerable mispricing of derivative instruments, especially out-of-the-money (OTM) options. To address these empirical limitations, there has been an increasing focus on enhancing the BSM framework to incorporate more realistic price dynamics. A particularly promising solution involves the application of Lévy processes. In contrast to Brownian motion, Lévy processes accommodate both continuous price changes and discrete jumps, thereby offering a more adaptable framework for modeling financial asset behavior. Introduced by Lévy (1937), these processes represent a category of stochastic models defined by independent and stationary increments, capable of capturing the heavy tails and asymmetry frequently observed in financial returns [4]. While Brownian motion is a specific instance of a Lévy process, the broader category permits a more complex dynamic structure, including the potential for jumps, which aligns more closely with the empirical characteristics of financial time series [3]. The initial notable utilization of Lévy processes within the realm of finance emerged with Mertons (1976) jump-diffusion model. This model enhanced the Black-Scholes-Merton (BSM) framework by integrating a Poisson jump process, thereby accommodating abrupt and infrequent fluctuations in asset prices. Mertons innovation was pivotal as it effectively represented discrete occurrences, such as market crashes or corporate announcements, which continuous models fail to adequately address. Nevertheless, despite its advancements over the BSM model by permitting jumps, the jump-diffusion model still operates under the premise that these jumps follow a Poisson process, implying that they are relatively uncommon and occur at a constant intensity. This premise constrains the model's capacity to accurately depict the heavy tails and frequent minor jumps that are characteristic of high-frequency financial data [9]. The constraints inherent in the jump-diffusion model prompted the creation of more advanced pure-jump Lévy models, which eliminate the continuous diffusion aspect entirely. A prominent example of such models is the Variance Gamma (VG) process, first proposed by Madan and Seneta (1990) and subsequently refined by Madan, Carr, and Chang (1998) [2]. The VG process is characterized as a pure jump model that accommodates a wide range of skewness and kurtosis, thus providing significant flexibility in modeling the empirical distribution of asset returns. In contrast to the BSM model, which presumes constant volatility, the VG model effectively captures the volatility smile observed in options markets, where implied volatility fluctuates with variations in strike price and maturity.

Expanding upon the VG process, Carr, Geman, Madan, and Yor (2002) introduced the CGMY model, which broadens the VG framework by accommodating both minor and significant jumps [1]. The CGMY model is classified within the

category of infinite activity Lévy processes. While Lévy models have been extensively studied over the past few decades, several challenges remain, particularly in terms of calibration and computational efficiency. Estimating the parameters of Lévy models from market data is not straightforward, especially due to the non-linearity of jumps and the infinite divisibility of Lévy processes. Recent research has focused on Fourier transform methods (Fang & Oosterlee, 2008) and machine learning techniques (Hernández et al., 2023) to improve the calibration process. However, there is still a need for further exploration into how these models perform in financial series prediction and their practical applications in vanilla option pricing [10] [5]. This study introduces novel contributions by investigating the performance of Lévy models in predicting asset price dynamics and their implications for the Black-Scholes model in predicting pricing of vanilla options. Specifically, we aim to compare the predictive accuracy of different Lévy models, including the Merton jump-diffusion, VG, and CGMY models, and assess their ability to price vanilla options under real market conditions. We also explore novel calibration techniques that leverage Fourier transform methods and optimization algorithms to improve the computational feasibility of using Lévy models in practice.

2 literature Review

The Black-Scholes Market Model

Investors are allowed to trade continuously up to some fixed finite planning horizon T . The uncertainty is modelled by a filtered probability space (Ω, \mathcal{F}, P) . A frictionless market with two assets is assumed. The first asset is one without risk (e.g:the bank account). Its price process is given by $B = \{B_t = \exp(rt), 0 \leq t \leq T\}$. The second asset is a risky asset, usually referred to as a stock, which pays a continuous dividend yield $q \geq 0$. The price process of this stock, $S = \{S_t, 0 \leq t \leq T\}$, is modelled by W , the geometric Brownian motion,

$$B_t = \exp(rt), \quad S_t = S_0 \exp\left(\left(\mu - \frac{1}{2}\sigma^2\right)t + \sigma W_t\right) \quad (1)$$

where $W = \{W_t, t \geq 0\}$ is a standard Brownian motion.

Note that, under P , W_t has a Normal($0, t$) and that $S = \{S_t, t \geq 0\}$ satisfies the stochastic differential equation. The parameter μ reflects the drift and σ models the volatility; μ and σ are assumed to be constant over time.

Generalities on Stochastic Processes

A family $(X_t)_{t \in \mathbb{R}^+}$ of random variables on a probability space $(\Omega, \mathcal{P}, \mathcal{F})$ is considered. A stochastic process can either be seen as a collection of distributions $(F_{X_t})_t$ of the random variables $(X_t)_t$ or as a mapping $t \mapsto X_t(\omega)$ for fixed $\omega \in \Omega$. In the latter case $X.(\omega)$ is called a path. In further investigating stochastic processes,

particularly with respect to the index set of time, we will be concerned with the information content in the market and the evolution of this information. To capture the revelation of information in a mathematically rigorous way we require the concept of filtration. A filtration $(\mathcal{F}_t)_t$ is a collection of σ -algebras such that $\mathcal{F}_s \subset \mathcal{F}_t \subset \mathcal{F}$, $s \leq t$.

The sigma algebra \mathcal{F}_t can be seen as the information available up to time t . A probability space obeying this property is called filtered probability space. We can then distinguish information currently available in the market from those which is still a possible scenario and therefore random. All this leads to study non anticipating processes. For a given filtration $(\mathcal{F}_t)_t$, i.e. an information structure, such a process is called adapted to the filtration if X_t is \mathcal{F}_t -measurable. An important property of this concepts a stochastic process is the martingale property. If the process (X_t) possesses this property, the best prediction of the future value of X_t at time $s < t$, $\mathbb{E}[X_t | X_s]$ is the present value X_s . The significance of this property in finance is manifold, as the No-Arbitrage Theory is based on this property and can allow computational probabilities calculated prior to investments in derivatives, and thus one could rely on Monte Carlo simulation methods to compute prices [21].

Brownian Motion

To treat Brownian motion mathematically, the mapping is considered

$$W : \mathbb{R}^+ \times \Omega \rightarrow \mathbb{R}; \quad (t, \omega) \mapsto W_t(\omega)$$

and $(W_t)_t$ is a Brownian motion if

(B1) starts at zero, i.e. $W_0 = 0$ for almost all $\omega \in \Omega$

(B2) has stationary independent increments

(B3) the distribution of $W(t)$ is Gaussian, $W_t \sim \mathcal{N}(0, t)$

(B4) the mapping $t \mapsto W_t(\omega)$ is continuous for almost all $\omega \in \Omega$.

Let shortly comment on the property (B2). Take arbitrary time points $\mathcal{T} := \{t_0, t_1, \dots, t_n\}$ such that $0 \leq t_0 \leq t_1 \leq \dots \leq t_n < \infty$. Then (B2) and (B3) state that $(W_{t_i} - W_{t_{i-1}})_{i=1, \dots, n}$ are independent Gaussian random variables and $W_{t+h} - W_t$ does not depend on h . The growth of Brownian motion therefore in each time interval $[S, T]$, $W(T) - W(S) \sim \mathcal{N}(0, T - S)$, only depends on the difference $T - S$. Adding a volatility σ changes the distribution to $\mathcal{N}(0, \sigma(T - S))$. This corresponds to the growth condition of a linear function in real analysis. Linear functions can be characterized by equal growth over time intervals with the same length. The expectation and the variance for this process are 0 and $\sigma^2 dt^2$ respectively. Furthermore, the volatility represented by the parameter σ can also be interpreted as a property of the path. It represents the quadratic variation, a measure of roughness of the path [17]. Figure 1 shows the distribution as well as typical paths of Brownian motion.

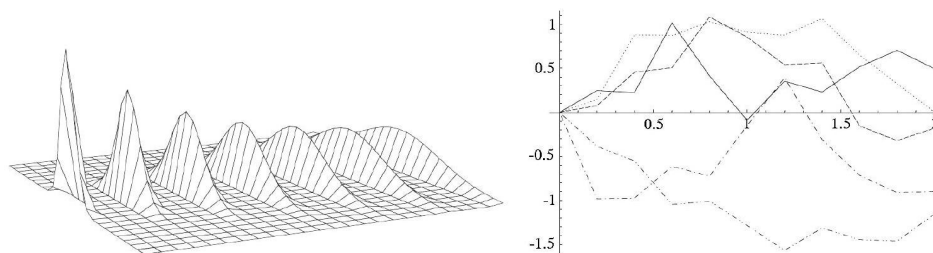


Figure 1: Illustration of a Brownian motion; distributions and paths

Poisson Process

By examining the Poisson process, an entirely distinct stochastic behavior is revealed. In contrast to Brownian motion it has discontinuous sample paths. It takes values in \mathbb{N} .

by considering a sequence of independent exponentially distributed random variables $(\tau_n), \tau_n \sim \mathbb{E}(\lambda), \lambda > 0$ and taking the sum $T_n := \sum_{i=1}^n \tau_i$ and by consider the following mapping

$$N : \mathbb{R}^+ \times \Omega \rightarrow \mathbb{N}; \quad N(t) \mapsto \sum_{n \geq 1} 1_{\{t \geq T_n\}} \quad (2)$$

$(N(t))_t$ is called Poisson process with intensity λ . This process is also known as counting process. It counts the random times T_n which occur between 0 and t .

(P1) starts at zero, $N(0) = 0$

(P2) has stationary, independent increments

(P3) the distribution of $N(T)$ is Poisson, i.e. $N(t) \sim \mathcal{P}(\lambda t)$.

(P4) the mapping $t \mapsto N(t)$ is piecewise constant and increases by jumps of size λ .

The Poisson process does not obey the martingale property but it is easy to make it into a martingale by subtracting the mean. The mean and variance are those of a Poisson distributed random variable and are both equal to λt . This leads to the compensated Poisson process which is given by $\tilde{N}(t) = N(t) - \lambda t$. The classical Poisson process can be obtained by setting $\lambda = 1$. A Compound Poisson process with intensity λ and jump size distribution J is a stochastic process given by 5

$$X(t) = \sum_{i=1}^{N(t)} Y_i(t) \quad (3)$$

where Y_i are independent and $Y_i \sim J$ and $N(t)$ being a Poisson process independent of $Y_i, i \in \mathbb{N}$

Similar to Brownian motion, the variance is of order dt . But this time the process jumps large distances only with small probability in time [19]. In Figure 2 the distribution and some typical path of the Poisson process is shown .

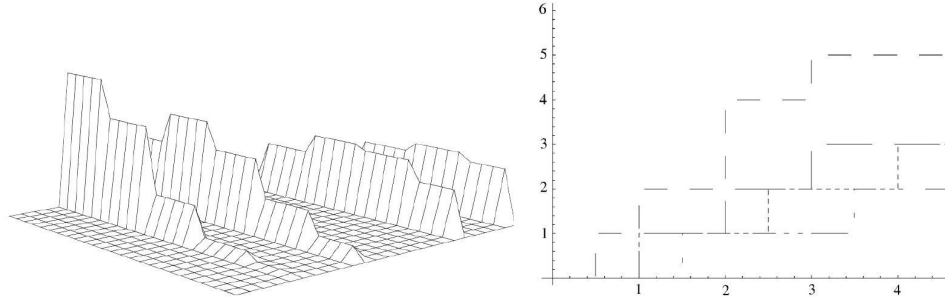


Figure 2: Illustration of a Poisson process; distributions and pathstext

Fourier transform

Indeed, each distribution is uniquely characterized by its characteristic function, which is the Fourier transform, and conversely. The sole requirement is the definition of the Fourier transform. For a given distribution F_{X_t} it is 6

$$\mathcal{F}(x) := \mathbb{E}_{F_{x_t}}[\exp(iux)] \quad (4)$$

If the distribution has a density f with respect to the Lebesgue measure the Fourier transform can be written as 7

$$\mathcal{F}(x) = \int_{\mathbb{R}^d} \exp(iux)f(u)du \quad (5)$$

Using that, the sum of independent identically distributed random variables is the product of the corresponding characteristic functions together with the independent increment property for a stochastic process and a time interval divided into n pieces of length dt gives (7)

$$\hat{F}_{X_t}(x) := \prod_{i=1}^n \hat{F}_{X_{dt}}(x) \quad (6)$$

Thus, to compute the Fourier transform of X_t it suffices to compute it for a small time interval of length dt [20].

By using the distribution of a Brownian motion to derive its characteristic function. We observe that the variance of W_{dt} is of order dt . Let \mathbb{P} be a probability measure with characteristic function $\hat{\mathbb{P}}$ For \mathbb{P} being the distribution of $\frac{X(t)}{\sqrt{dt}}$ then $\hat{X}_{dt}(u) = \hat{\mathbb{P}}(u\sqrt{dt})$. Since the expectation of $X(t)$ is 0 we have $\int_x \mathbb{P}(dx) = 0$. Using that $\hat{\mathbb{P}}$ is the Fourier transform of a probability measure and expanding it into a Taylor series we obtain

This corresponds to a small movement over small time intervals with high probability which is illustrated in Figure 3.

$$\hat{X}_{dt}(u) \approx 1 + \frac{\overbrace{\hat{\mathbb{P}}^{(2)}(0)}{=\sigma}}{2} u^2 dt \approx \exp\left(-\frac{u^2 \sigma dt}{2}\right)$$

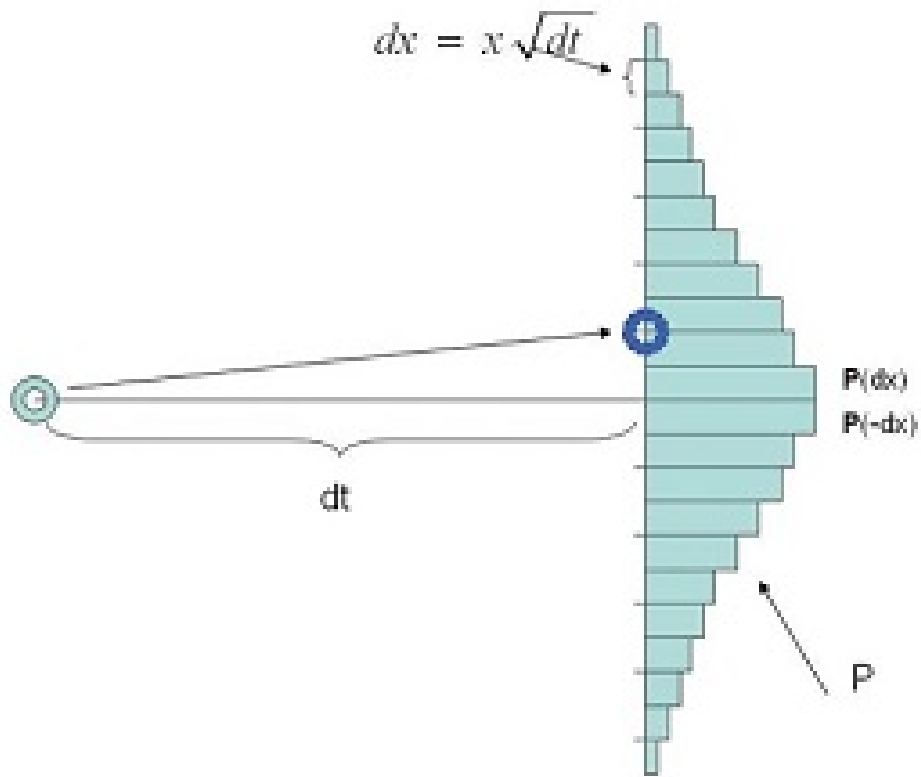


Figure 3: Computing Fourier Transform for a Brownian motion

There is yet another way for a stochastic movement represented by a Poisson process. This is a big move over small time intervals with low probability. To study this movement, the characteristic function of a Poisson process is derived. To this end, consider a process which jumps from its current state on the interval dt to a level x with probability λ and stays at its current state with probability $1 - \lambda$.

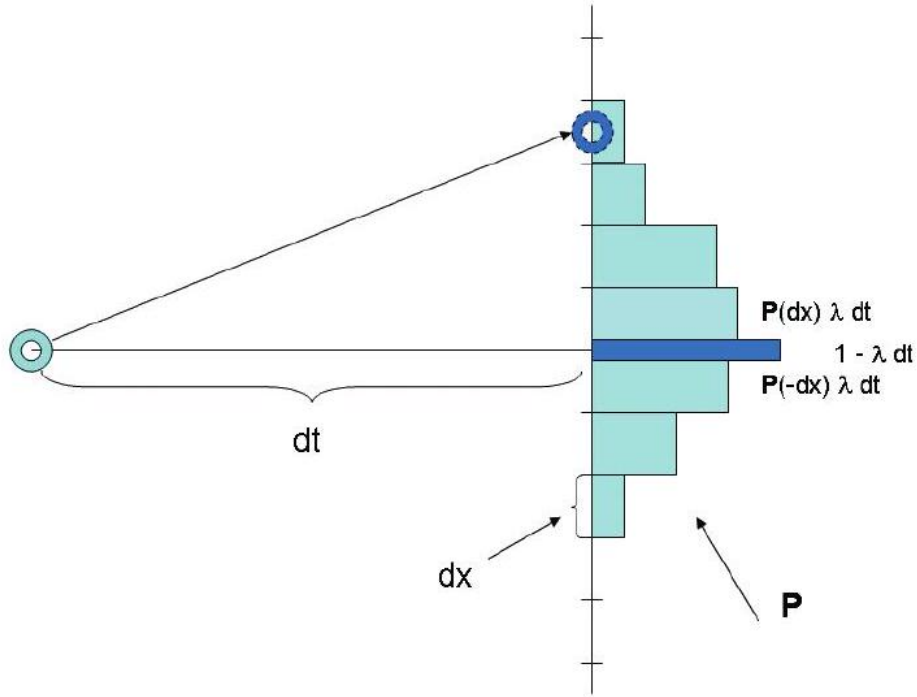


Figure 4: Computing Fourier transform for a Poisson process

Therefore, the characteristic function can be easily computed and is [13]

$$\hat{X}_{dt}(u) = \lambda dt e^{iux} + (1 - \lambda) e^0 = 1 + (e^{iux} - 1) \lambda dt \approx \exp((e^{iux} - 1) \lambda dt) \quad (7)$$

$\hat{X}_t(u) = \hat{X}_{dt}(u)^{t/dt}$ holds by multiplication using (P2) and leads to

$$\hat{X}_t(u) = \exp(\exp(e^{iux} - 1) \lambda t) \quad (8)$$

Thus, the characteristic function of the Poisson process by setting $x = 1$ and $\lambda = 1$ is recovered, hence

$$\mathbb{E} \left[e^{iuN(t)} \right] = \exp(\lambda t (e^{iu} - 1)). \quad (9)$$

Figure 4 illustrates the calculation and the stochastic movement of the Poisson process.

It is now easy to construct a process having jump size x and jump probability λ . This corresponds to multiplication of the Poisson process $N(t)$ by x and exchange t by λt .

It is possible to derive distributional properties as well. The moments of the distribution can, for instance, be computed through differentiation.

Lèvy Processes

A closer look at the properties of Brownian motion and Poisson motion reveals that they obey the following similarities:

(L1) starts at 0

(L2) has stationary, independent increments

(L3) has stationary increments, i.e. the distribution of $X(t+h) - X(t)$ does not depend of h

(L4) is stochastically continuous, i.e. for all ϵ , $\lim_{h \rightarrow 0} P(|X_{t+h} - X_t| \geq \epsilon) = 0$

The processes only differ in the distribution, Gauss and Poisson, and the path properties, continuous and piece-wise constant. If we take the properties (L1) to (L4) as the definition of a class of stochastic processes, called Levy processes. Brownian and Poisson processes are members of that class. In fact, we can interpret this class as a stochastic analogue of a linear function. The property (L2) can be seen as the stochastic analogue of the equal growth condition. Different linear functions are governed by different constant growth rates. Their stochastic counterparts obey the different distributions [18]. The stochastic counterpart has numerous properties which can all be studied by examining the characteristic function. We have already seen that the processes considered above are fundamental building blocks of a general class, as the next section will show.

The Lèvy Khinchine Theorem

In fact, the characteristic function of a general Lèvy process can be derived. This is the Lèvy Khinchine Theorem. For a fixed Lèvy measure F we denote $h(x) := x1_{\{|x| \leq 1\}}$ and $b_{Fh} := b + \int h(x)F(x)$. Then we have the Fourier transform of the Lèvy process $(X_t)_{t \in \mathbb{R}^+}$ [16]

$$\hat{X}_t(u) = \exp\left(\underbrace{iub_{Fh}}_{\text{drift}} - \underbrace{1/2u^2\sigma}_{\text{diffusion}} + \underbrace{\int (e^{iux} - 1 - iuh(x)) F(dx)}_{\text{jump}}\right) t \quad (10)$$

What does the formula tell and how does a Lèvy process actually move? First of all, we see that the Lèvy process is determined by fixing the function b , the measure F and the parameter σ . A triple (b_{Fh}, σ, F) is called Lèvy triplet. To further shed light on the above question we have to study all the components which constitute the characteristic function given in the Lèvy Khinchine Theorem. Firstly, we interpret the Lèvy measure F as a generalization of the measure \mathbb{P} used for illustrating the stochastic movements from above. By the usual convention, we will consider jumps of height bigger than 1 as big jumps. Let us further examine the movement of a general Lèvy process. The drift and diffusion parts of (10) are the characteristic functions of a linear function and a Brownian motion respectively. Let us have a closer look at the jump component [14]

$$u \mapsto (\exp(-iux) - 1 - iuh(x))F(dx)t \quad (11)$$

Processes with such characteristic function are pure jump processes. The parameter x is the jump height and $F(dx)$ is the jump intensity. We already considered a pure jump process, the Poisson process. We examine how this process fits in here and what does happen if the jumps occur too frequently or the jump size is too big?

Why is the function chosen as in (10)? If we had chosen $h(x) = 0$ in the general setting and F as the measure \mathbb{P} from the beginning, we would see that the simple Poisson process fits into the above framework. The compensated Poisson process can also be considered by setting $h(x) = x$. For a general function h we also get a process which is x times a Poisson process compensation by a linear function. But it is only partially compensated if $0 < h(x) < x$.

But there are processes which would not lead to definite integrals in (10). These are processes with too big or too many jumps. The jump size too big means mathematically that [11]

$$\int_{\{|x|>1\}} |x|F(dx) = \infty \quad (12)$$

The (12) indicates that the jump sizes that are larger than 1 have a significant impact on the stochastic process being considered. Specifically, the integral diverging to infinity means that there are sufficiently large jumps in the process that occur frequently enough to have a substantial effect. In other words, if you sum up the sizes of all the jumps greater than 1 (weighted by their likelihood according to the distribution F), you end up with an infinite value. This suggests that the process experiences "big jumps" that can dominate its behavior.

Too many small jumps means mathematically that

$$\int_{\{|x|\leq 1\}} x^2 dF(x) = \infty \quad (13)$$

The (13) indicates that the cumulative contribution of all jump sizes within the range of -1 to 1 is infinite when weighted by the square of the jump sizes x^2 . This scenario represents a condition of "too many small jumps." It suggests that while the individual jumps are small (within the absolute bounds of 1), their frequency and the way they accumulate (given that we're using x^2 , which accentuates the effect of larger small jumps) result in an infinite aggregate impact on the process.

Therefore, for such processes we have to cut-off with h . If we now consider the general setting with a function h then the corresponding jump process could also be seen as a compensated Poisson process perturbed by a linear function, but the expectation will only be compensated for a value between 0 and 1.

With the general formula at hand, we can find out about the behavior of sample paths. It is differentiable if and only if $\sigma = 0$ and $F = 0$. Continuity is a property

of a diffusion and can only be achieved if $F = 0$ otherwise there are jumps leading to discontinuities. If we have a jump part then there occur finitely many jumps in finite intervals if $F([-1, 1]) < \infty$. Otherwise there are infinitely many. We only have a path of finite variation if $\int_{|x| \leq 1} |x|F(dx) < \infty$

Distributional properties like the moments of the distribution of $X_t, t \in \mathbb{R}^+$, can be computed by differentiation and are given by 8 [12]

$$m_k := \mathbb{E}[X^k] = \frac{1}{i^k} \frac{\partial^k \mathcal{F}(x)}{\partial x^k}(0) \quad (14)$$

Thus,

$$\begin{aligned} \mathbb{E}[X(t)] &= t \cdot \left(b + \int_{\{|x| \geq 1\}} xF(dx) \right); \mathbb{V}[X(t)] = t \cdot \left(\sigma + \int x^2 F(dx) \right) \\ \mathbb{S}[X(t)] &= \frac{t \int x^3 F(dx)}{(t \int x^2 F(dx))^{\frac{3}{2}}}; \mathbb{K}[X(t)] = \frac{t \int x^4 F(dx)}{(t \int x^2 F(dx))^2} \end{aligned} \quad (15)$$

Notice that the distributional properties are determined by the shape of the Lévy measure for big $|x|$ whereas the path properties are determined by the small $|x|$. Thus, a Lévy process can be constructed using three components. The stochastic components correspond to two ways of stochastic movement discussed above.

Methodology

The dataset consists of 77 mid-prices of a set of European call options on the S&P 500 Index at the close of the market on 11 April 2022. On this day the S&P 500 closed at 4412.53. Since, by the put-call parity, the price of a put option can be calculated from the price of the call option with the same strike and maturity, and vice versa, we include in our set only call option prices. The data was collected from the Yahoo finance site and the analysis was done with Python software along with financial packages.

The option prices can be visualized as in Figure 5, which shows several series of call options. The upper series consists of options with the highest time to maturity corresponding to options expiring in December 2023. The inner series consists of options expiring in May 2022, June 2022, September 2022, December 2022, March 2023 and finally in June 2023. We will calibrate different models to this set. The market prices are always denoted by a circle and later on the model prices will be denoted by a plus sign. It is the goal to calibrate the model such that plus signs shoot right through the middle of the corresponding circles.

The parameters coming out of the calibration procedure resemble the current market view on the asset. Here we do not explicitly take into account any historical data. All the necessary information is contained in today's option prices, which we

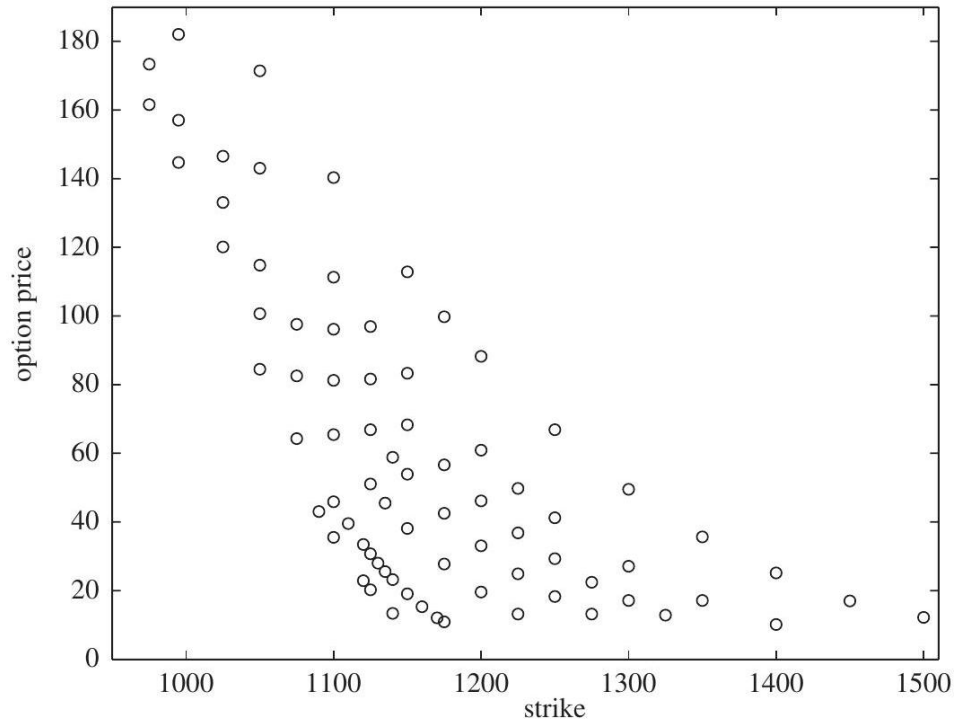


Figure 5: S&P 500 market option prices

observe in the market. Using the available pricing techniques, this method is useful for pricing derivatives, such as OTC options, whose prices are not available in the market and for finding mispricings in a set of European vanilla options.

APE, AAE, RMSE and ARPE

For comparative purposes, we compute the average absolute error as a percentage of the mean price. This statistic, which we will denote by APE, is an overall measure of the quality of fit

$$\text{APE} = \frac{1}{\text{mean option price}} \sum_{\text{options}} \frac{|\text{market price} - \text{model price}|}{\text{number of options}} \quad (16)$$

Other measures which also give an estimate of the goodness of fit are the average absolute error (AAE), the average relative percentage error (ARPE) and the root mean-square error (RMSE)

$$\begin{aligned}
\text{AAE} &= \sum_{\text{options}} \frac{|\text{market price} - \text{model price}|}{\text{number of options}} \\
\text{ARPE} &= \frac{1}{\text{number of options}} \sum_{\text{options}} \frac{|\text{market price} - \text{model price}|}{\text{market price}} \\
\text{RMSE} &= \sqrt{\sum_{\text{options}} \frac{(\text{market price} - \text{model price})^2}{\text{number of options}}}
\end{aligned} \tag{17}$$

As a general rule, we estimate the model parameters by minimizing the root-mean-square error between model prices and market prices. We will attempt to model stock-price behavior using a more sophisticated stochastic process than the Brownian motion of the BlackScholes model. The stock-price dynamics are now represented by a Lévy process, allowing us to model stock prices as the exponential of this Lévy process. We can incorporate skewness and excess kurtosis, and we will demonstrate that we can fit our underlying distributions to historical data quite accurately. Next, we will price European options under our model. Finally, we will calibrate our model to a set of available market option prices. We should observe a significant improvement compared to the BlackScholes model.

Statistical Testing

We fit the Meixner distribution to several datasets, which we have already encountered of daily log returns of S&P index. By this, we illustrate that the more flexible distributions, such as the Meixner, are more suitable than the normal distribution. We assume that we have n independent observations x_1, \dots, x_n of a random variable X . Typically, these observations will be the log returns of our financial asset. From these observations, we would like to deduce reasonable estimators for the parameter set θ . Note that under a Lévy process setting, the log returns over non overlapping intervals of fixed length (typically, one day) will be independent and identically distributed [9]. Sometimes, adhoc methods can also deliver reasonable estimators. However, we give an overview of the classical maximum-likelihood estimation method.

The maximum-likelihood estimator (MLE) $\hat{\theta}_{\text{MLE}}$ is the parameter set that maximizes the likelihood function

$$L(\theta) = \prod_{i=1}^n f(x_i; \theta) \tag{18}$$

Thus, we choose values for the parameters that maximize the chance (or likelihood) of the data occurring.

Maximizing an expression is equivalent to maximizing the logarithm of the expression, and this is sometimes easier. So, we sometimes maximize the log likelihood

function,

$$\log L(\theta) = \sum_{i=1}^n \log f(x_i; \theta) \quad (19)$$

To maximize the (log)-likelihood function, we often have to rely on numerical procedures; however, in a few cases these estimators can be calculated explicitly. The MLE estimators for the mean and variance of the Normal distribution are given by the sample mean and sample variance

$$\hat{\mu}_{\text{MLE}} = \frac{1}{n} \sum_{i=1}^n x_i, \quad \hat{\sigma}_{\text{MLE}}^2 = \frac{1}{n} \sum_{i=1}^n x_i^2 - \left(\frac{1}{n} \sum_{i=1}^n x_i \right)^2 \quad (20)$$

3 Main results

Density and Log Density Fits

Figure 6 shows the Gaussian kernel density estimator based on the daily log returns of the S&P 500 Index over the period from 2001 until the end of 2021, together with the fitted Meixner distribution, with parameters from Table 1. Compared with the normal counterpart, we see a significant improvement. Note also that the Meixner distribution has semi-heavy tails and as such is capable of also fitting the tail behavior quite well. This can be seen from the log density plot in Figure 6.

Table 1: Meixner χ^2 -test: MLE parameters and P -values

Index	a	b	d	m	P_{Meixner} -value
S&P 500 (2001-2021)	0.0204	-0.0829	0.4140	0.0006	0.4754

χ^2 -Tests

For the χ^2 -tests we take the same intervals as when the normal distribution. Parameters are estimated by the MLE method. In the Meixner case, four parameters have to be estimated, so we take $n - 5$ degrees of freedom (n is the number of observations).

Table 1 shows the values of the P -values of the χ^2 -test statistic with equal width for the Meixner null hypothesis. Recall that we reject the hypothesis if the P -value is less than our level of significance, which we take to be 0.05, and accept it otherwise.

We see that the Meixner hypothesis is accepted and yields a very high P -value.

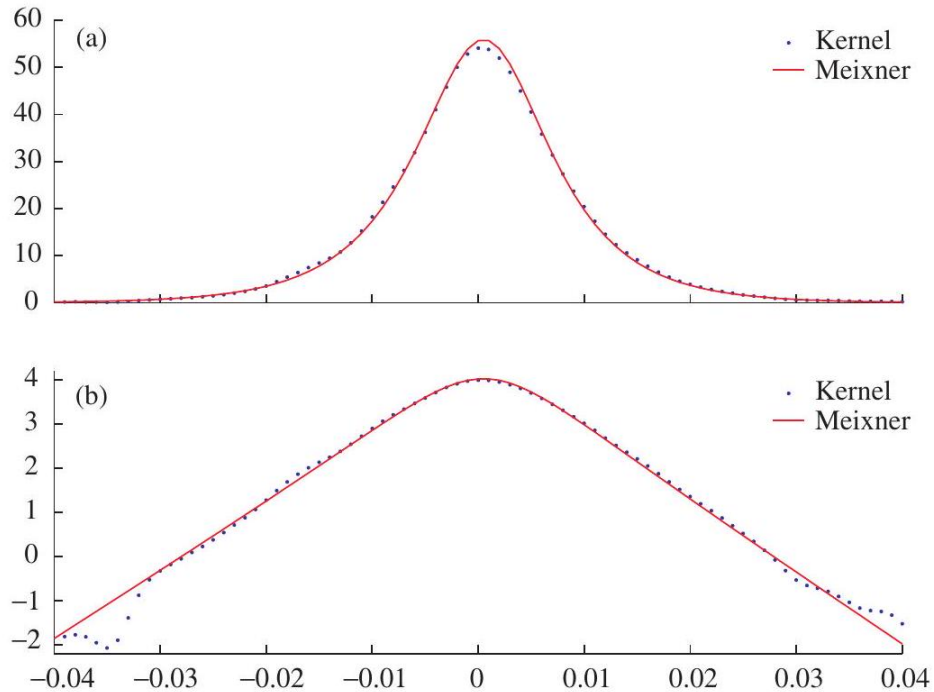


Figure 6: (a) Meixner density and Gaussian kernel density estimators and (b) log densities of the daily log returns of the S&P 500 Index

Pricing Formulas for European Options

Given our market model, we focus now on the pricing of European options for which the payoff function is only a function of the terminal stock price, i.e. the stock price S_T at maturity T : $G(S_T)$ denotes the payoff of the derivative at its time of expiry T i.e. $F(X_T) = G(S_0 \exp(X_T))$. In the case of the European call with a strike price K , we have $G(S_T) = (S_T - K)^+$ and $F(X_T) = (S_0 \exp(X_T) - K)^+$ [6].

Pricing through the Lévy Characteristics

In all cases where the underlying process is a Lévy process (for simplicity without a Brownian component) in the risk-neutral world and the price $V_t = V(t, X_t)$ at time t of a given derivative satisfies some regularity conditions (i.e. $V(t, x) \in C^{(1,2)}$), the function $V(t, x)$ can also be obtained by solving a partial differential integral

equation (PDIE) with boundary condition, all in the Lévy characteristics [8]

$$rV(t, x) = \gamma \frac{\partial}{\partial x} V(t, x) + \frac{\partial}{\partial t} V(t, x) + \int_{-\infty}^{+\infty} \left(V(t, x + y) - V(t, x) - y \frac{\partial}{\partial x} V(t, x) \right) \nu_Q(dy)$$

$$V(T, x) = F(x) \tag{21}$$

where $[\gamma, 0, \nu_Q(dy)]$ is the triplet of Lévy characteristics of the Lévy process under the risk-neutral measure Q . This PDIE is the analogue of the famous BlackScholes PDE and follows from the FeynmanKac formula for Lévy processes. It was derived from Nualart and Schoutens (2001) and Raible (2000).

3.1 Calibration of Market Option Prices

The parameters which should resemble the markets view on the asset can be found through a calibration procedure on the markets option prices themselves. Here we do not explicitly take into account any historical data. All necessary information is contained in todays option prices, which we observe in the market. We estimate the model parameters by minimizing the root-mean-square error between the markets and the models prices.

If we choose the mean-correcting equivalent martingale measure, we obtain a calibration for the Meixner model in Figures 7. In Table 2 the parameters coming from the calibration procedure are given.

Table 2: Lévy models (mean correcting): parameter estimation

Model	parameters		
Meixner	α	β	γ
	.455	-1.552	.45

In Table 3 the relevant values of APE, AAE, RMSE and ARPE are given. Basically, the four-parameter models perform better than the less-parameter models. Based on this calibration. This calibration is momentary and we typically see that calibrations to other datasets (of different underlies or on different times in history) can favor the model that performs better.

Table 3: Lévy models (mean-correcting): APE, AAE, RMSE, ARPE.

Model	APE(%)	AAE	RMSE	ARPE(%)
Meixner	4.23	2.654	3.345	6.92

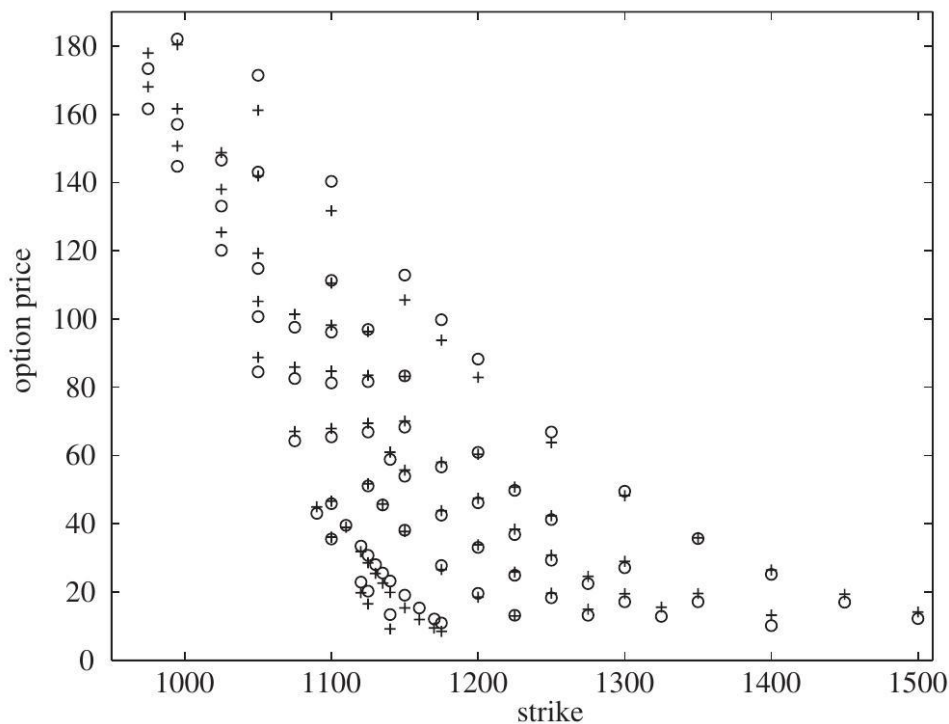


Figure 7: Meixner (mean-correcting) calibration of S&P 500 options (circles are market prices, pluses are model prices).

4 results and recommendation

For the model considered, closed form expressions for the characteristic function of the log price process were given. The models involved were calibrated to market option prices and were capable of adequately fitting option prices over a wide range of strikes and maturities. We see an improvement over the BlackScholes prices. However, we still observe a significant difference from real market prices. It is typical that Lévy model incorporates a smile effect, although the effect does not completely correspond with the market. Moreover, there is evidence that the Lévy mexiner model is much more reliable; it gives a much better indication of the true price than the pure BlackScholes model. These almost perfect representations of the vanilla option surface lead to interesting applications for the pricing of exotic options. Then in In future studies, it is suggested to use other derivatives such as exotic and American options or interest rate models for testing. Also, other processes like The Generalized Hyperbolic Process and The Variance Gamma Process could be used to estimate the model and compare the results.

Bibliography

- [1] Peter Carr, Hélyette Geman, Dilip B Madan, and Marc Yor, *Stochastic volatility for lévy processes*, *Mathematical finance* **13** (2003), no. 3, 345–382.
- [2] Peter Carr and Liuren Wu, *The finite moment log stable process and option pricing*, *The journal of finance* **58** (2003), no. 2, 753–777.
- [3] Rama Cont, *Empirical properties of asset returns: stylized facts and statistical issues*, *Quantitative finance* **1** (2001), no. 2, 223.
- [4] Nathalie Eisenbaum, Andreas Kyprianou, Ana-Maria Matache, and Goran Peskir, *Local time-space calculus with applications*, *SIAM Journal of Control and Optimization* (2003), 1343.
- [5] Fang Fang and Cornelis W Oosterlee, *A novel pricing method for european options based on fourier-cosine series expansions*, *SIAM Journal on Scientific Computing* **31** (2009), no. 2, 826–848.
- [6] John C Hull and Sankarshan Basu, *Options, futures, and other derivatives*, Pearson Education India, 2016.
- [7] Zuzana Janková, *Drawbacks and limitations of black-scholes model for options pricing*, *Journal of Financial Studies and Research* **2018** (2018), 1–7.
- [8] Jorge A León, Josep L Solé, Frederic Utzet, and Josep Vives, *On lévy processes, maliavin calculus and market models with jumps*, *Finance and Stochastics* **6** (2002), 197–225.
- [9] Dilip B Madan and Marc Yor, *Representing the cgmy and meixner lévy processes as time changed brownian motions*, *Journal of Computational Finance* **12** (2008), no. 1, 27.
- [10] Alejandro Morales-Hernández, Inneke Van Nieuwenhuyse, and Sebastian Rojas Gonzalez, *A survey on multi-objective hyperparameter optimization algorithms for machine learning*, *Artificial Intelligence Review* **56** (2023), no. 8, 8043–8093.
- [11] Ernesto Mordecki, *Optimal stopping and perpetual options for lévy processes*, *Finance and Stochastics* **6** (2002), 473–493.
- [12] David Nualart and Wim Schoutens, *Chaotic and predictable representations for lévy processes*, *Stochastic processes and their applications* **90** (2000), no. 1, 109–122.
- [13] Bernt Øksendal and Frank Proske, *White noise of poisson random measures*, *Potential Analysis* **21** (2004), 375–403.
- [14] Jan Rosiński, *Series representations of lévy processes from the perspective of point processes*, *Lévy processes: theory and applications*, Springer, 2001, pp. 401–415.
- [15] Boris Salazar, *Mandelbrot, fama and the emergence of econophysics*, *Cuadernos de Economía* **35** (2016), no. 69, 637–662.
- [16] René L Schilling, *An introduction to lévy and feller processes*, *Lévy-type processes to parabolic SPDEs*. Birkhäuser, Cham (2016), 1–30.
- [17] F Shokrollahi, D Ahmadian, and LV Ballestra, *Pricing asian options under the mixed fractional brownian motion with jumps*, *Mathematics and Computers in Simulation* **226** (2024), 172–183.
- [18] W Shoutens, *Lévy processes in finance*, 2003.
- [19] Ritik Soni and Ashok Kumar Pathak, *Generalized iterated poisson process and applications*, *Journal of Theoretical Probability* (2024), 1–30.
- [20] Seyed Jalal Tabatabaei and Alireza Pakgozar, *Time series modeling of extreme losses values based on a spectral analysis approach*, *Financial Research Journal* **22** (2021), no. 4, 594–611.
- [21] Peter Tankov, *Financial modelling with jump processes*, Chapman and Hall/CRC, 2003.

How to Cite: Seyed Jalal Tabatabaei¹, *Stochastic portfolio optimization by diversity-weighted portfolio approach*, *Journal of Mathematics and Modeling in Finance (JMFM)*, Vol. 4, No. 2, Pages:65–82, (2024).



The Journal of Mathematics and Modeling in Finance (JMFM) is licensed under a Creative Commons Attribution NonCommercial 4.0 International License.